Physics Letters B 763 (2016) 422–426

Contents lists available at ScienceDirect

Physics Letters B

www.elsevier.com/locate/physletb

Exclusive measurement of isospin mixing at high temperature in ^{32}S

Debasish Mondal [a,b], Deepak Pandit [a], S. Mukhopadhyay [a,b], Surajit Pal [a], Srijit Bhattacharya [c], A. De [d], Soumik Bhattacharya [a,b], S. Bhattacharyya [a,b], Balaram Dey [e], Pratap Roy [a,b], K. Banerjee [a,b], S.R. Banerjee [a,b,*]

[a] Variable Energy Cyclotron Centre, 1/AF-Bidhannagar, Kolkata-700064, India
[b] Homi Bhabha National Institute, Training School Complex, Anushaktinagar, Mumbai-400094, India
[c] Department of Physics, Barasat Government College, Kolkata-700124, India
[d] Department of Physics, Raniganj Girls' College, Raniganj-713358, India
[e] Tata Institute of Fundamental Research, Mumbai-400005, India

ARTICLE INFO

Article history:
Received 5 August 2016
Received in revised form 5 October 2016
Accepted 25 October 2016
Available online 2 November 2016
Editor: V. Metag

Keywords:
Isospin mixing in nuclei
Isovector giant dipole resonance
Statistical theory of nucleus
BaF_2 detectors

ABSTRACT

Exclusive measurement of isospin (I) mixing in ^{32}S at high temperature (T) has been performed utilizing the γ-decay of isovector giant dipole resonance (IVGDR). The degree of isospin mixing was deduced from the ratio of high energy γ-ray cross-sections of ^{32}S and ^{31}P populated at the same temperature and angular momentum (J). Precise temperature was determined by simultaneous measurement of nuclear level density (NLD) parameter and angular momentum. The measured Coulomb spreading width ($\Gamma^{\downarrow}$) seems to be independent of temperature and angular momentum. The isospin becomes a good quantum number with increase in temperature. However, when compared with the calculation at high temperature, measured isospin mixing is underpredicted by the calculations.

The concept of charge symmetry and charge independence is formalized via the concept of isospin quantum number I [1,2]. It is fully preserved by the charge independent part of nuclear interaction. However, the presence of electromagnetic interactions and the charge dependent short range potential break the isospin symmetry in nuclei; the most important part being the isovector Coulomb interaction which mixes states separated by $\Delta I = 1$ [3]. Despite being a small effect, isospin mixing is important in connection with two basic phenomena in physics, namely, the spreading width of isobaric analog states (IAS) [4–6] and the superallowed Fermi β-decay [7–10]. The spreading width of the IAS is directly related to the isospin mixing in the parent nuclei [5,6]. While, in case of superallowed Fermi β-decay, the measured lifetime is related to the vector coupling constant G_V which in turn is crucial in determining the u-quark to d-quark transition matrix element V_{ud} in the Cabibbo–Kobayashi–Maskawa (CKM) matrix. However, the measured ft value needs several corrections [7]; one of them being δ_c, which is related to the isospin mixing [9]. In recent years, experimental advances have put the theoretically calculated corrections under intense scrutiny.

In general, isospin mixing can be studied by utilizing the transitions which would have been forbidden if isospin mixing does not take place. For example, a) electric dipole transition in self conjugate nuclei [11], b) Fermi β-decay [12,13], c) splitting of the IAS studied by β delayed γ-rays [14] and d) evaporated $E1$ γ-rays from the decay of IVGDR [15].

At moderate excitation energies the γ-rays associated with the decay of IVGDR are emitted mostly from the first stage of the compound nuclear decay. It is, therefore, an ideal tool to study the isospin mixing in self conjugate (N = Z) nuclei in the excitation energy range where the statistical model of nuclei can be applied. Owing to the isovector nature of the decay, the γ-transitions between the states of same I are forbidden in N = Z nuclei. Consequently, if a self-conjugate nucleus is populated by bombarding a self-conjugate projectile on a self-conjugate target, only I = 0 states are populated in the compound nucleus (CN) with the assumption that the isospin is fully conserved. Due to the above mentioned isospin selection rule γ-transitions only between states I = 0 to I = 1 are allowed. But, at moderate excitation energies there are not many I = 1 final states to be populated by IVGDR γ-decay. This results in the suppression of the yield of γ-rays decaying from self-conjugate nuclei populated through

* Corresponding author at: Variable Energy Cyclotron Centre, 1/AF-Bidhannagar, Kolkata-700064, India.
E-mail address: srb@vecc.gov.in (S.R. Banerjee).

http://dx.doi.org/10.1016/j.physletb.2016.10.065

$I = 0$ entrance channel as compared to I $\neq$ 0 nuclei for which all γ-transitions are allowed. However, in presence of an admixture of I = 1 states in the initial compound nucleus, the IVGDR γ-yield is enhanced as these I = 1 states can decay to I = 0 states.

The above technique was first proposed by Harakeh et al. [15] and was later modified by Behr et al. [16] who formalized the isospin mixing as prescribed in Ref. [17]. It was shown, by inclusive high energy γ-ray measurement, that for ^{28}Si isospin gradually becomes a good quantum number as excitation energy increases. Recently, isospin mixing has been measured for ^{80}Zr [18,19]. They concluded that the Coulomb spreading width ($\Gamma^{\downarrow}$), in fact, remains constant with temperature and isospin mixing decreases with the increase in temperature. The result was compared with the calculation of Sagawa et al. [6] who proposed that the spreading width of the IAS arises due to the coupling of isovector monopole (IVM) states and they connected the isospin mixing in the parent nucleus to the spreading width of the IAS. Interestingly, the result matches well with the calculation; also when extrapolated to zero temperature, the result agrees quite well with the recent calculation of Satula et al. [20]. However, at lower mass regions the measured isospin mixing values seem to be a bit higher at higher temperatures [21]. It could also be mentioned here that in all the measurements which applied the formalism of Ref. [16] to extract isospin mixing, heavy ion fusion reaction was used to ensure the statistical nature of the evaporated γ-rays. However, in such reactions the compound nuclei are populated at higher angular momenta which in turn affect the high energy γ-ray spectrum [22], particularly at lower mass regions [23]. It should also be pointed out that in all the previous measurements in lower mass regions the nuclear level density (NLD) parameter, which is vital for statistical model calculations as well as for precise determination of nuclear temperature, was not measured.

In this letter, we report on the measurement of isospin mixing in ^{32}S for which only one measurement exists at 58.3 MeV [24]. Our primal objectives were to a) populate the compound nucleus with light ion (α) induced fusion reaction to minimize the angular momentum effect; these reactions have been extensively used to study the low temperature properties of IVGDR [25–27], b) precisely measure the angular momentum populated by measuring the low energy γ-ray multiplicity, c) measure the crucial NLD parameter, for the first time in this context, by measuring the evaporated neutron energy spectrum, d) determine the exact temperature by simultaneous measurement of angular momentum and NLD parameter, e) compare our result with the calculations of Ref. [6] and attempt to extrapolate the result towards zero temperature.

The experiments were performed at the Variable Energy Cyclotron Centre (VECC), Kolkata. The compound nuclei ^{31}P and ^{32}S were populated at the same excitation energy (E* = 40.2 MeV) and angular momentum ($< J >= 12\hbar$) through I = 1/2 and I = 0 entrance channels by bombarding self-supporting ^{27}Al (I = 1/2) and ^{28}Si (I = 0) target nuclei with α-beam (I = 0) of energies 35 MeV and 38 MeV, respectively from K-130 Cyclotron. The target thicknesses were 7.1 and 10.8 mg/cm^2 for ^{27}Al and ^{28}Si, respectively. Here ^{31}P was populated as a reference nucleus (populated through different entrance channel isospin but at same E* and $< J >$) to find the IVGDR parameters (energy, width and strength) to be used for the analysis of ^{32}S. As the masses of the two compound nuclei are nearly same and they are populated at the same excitation energy and angular momentum, IVGDR parameters are expected to be same for both the nuclei. It should also be mentioned that the critical angular momentum (J_c) [28], above which noticeable effect on IVGDR width is observed, is 11$\hbar$ for ^{32}S. Consequently, the high energy γ-ray spectra are expected to be sensitive to temperature only.

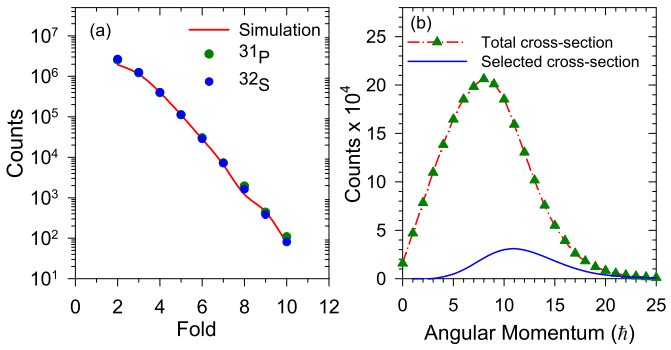

Fig. 1. (Color online.) (a) Experimental fold distributions along with the simulated one. (b) The total fusion cross-section (arb. unit) (green solid triangles with red dot-dashed line) and the selected angular momentum distribution (solid blue line) for CASCADE calculations.

The high energy γ-ray spectra from the decay of IVGDR were measured using a part of the LAMBDA spectrometer [29]. A total of 49 BaF_2 detectors, each having dimension of 3.5 × 3.5 × 35 cm^3, were arranged in a 7 × 7 matrix. The detector system was placed at a distance of 50 cm from the target and at an angle of 90° with respect to the beam axis. The geometrical efficiency of the system was 1.8%. It was surrounded by a 10 cm thick passive lead shield to block the γ-ray backgrounds. A 50 element multiplicity filter (BaF_2 detector each having dimension of 3.5 × 3.5 × 5.0 cm^3) was also utilized for precise measurement of angular momentum populated as well as to take start trigger for time of flight (TOF) measurements. The multiplicity filter was divided into two parts of 25 elements each and they were placed on top and bottom of the target chamber in 5 × 5 matrix at a distance of 5 cm from the target. To ensure equal solid angle for each detector, each matrix was configured in a staggered castle type geometry. The data were acquired using a VME based data acquisition system. Only those events for which at least one detector from both the top and bottom multiplicity filters fired in coincidence with one of the BaF_2 detectors of LAMBDA spectrometer above a threshold of 4.0 MeV were recorded. This coincidence technique, despite selecting the higher angular momentum phase space (Fig. 1b), guarantees the selection of statistical events as well as a significant reduction in background events. The neutron events were rejected by using TOF technique and the pulse shape discrimination (PSD) technique was utilized to get rid of the pile-up events in each detector by measuring the charge deposition over two integrating time intervals of 50 ns and 2 µs. The time spectrum of the cyclotron radio frequency (RF) was also recorded with respect to the multiplicity filter to further ensure the selection of beam related events. The high energy γ-ray spectra were reconstructed using cluster summing technique [29] in which each detector was required to satisfy the prompt time gate and PSD gate. The events were so selected that they should lie within the prompt gate of RF time spectrum.

The evaporated neutron energy spectra were measured, in coincidence with the multiplicity γ-rays, using a liquid scintillator based neutron TOF detector [30]. It was placed at an angle of 150° with respect to the beam axis and at a distance of 150 cm from the target. The $n-\gamma$ discrimination was done using PSD technique comprising of TOF and zero crossover time (ZCT). The TOF spectra were converted to neutron energy spectra using the prompt γ-peaks in the TOF as time reference. The energy spectra were converted from laboratory frame to center of mass (CM) frame. The energy resolution of the present set-up is ∼17% at 1 MeV. The detailed energy dependent neutron detection efficiency can be found in Ref. [30]

The angular momenta populated in the reactions studied do not affect the IVGDR parameters considerably. However, to determine the temperature of the compound nuclei, it is important to determine the angular momentum accurately; also the selection of proper angular momentum phase space (as we have selected only those events for which both of the top and bottom multiplicity filters fired in coincidence) is crucial for statistical model calculations. Thus the experimentally measured fold distribution was mapped into angular momentum space with Monte Carlo GEANT3 simulations [31]. The detailed procedure can be obtained in Ref. [32]. The experimental fold distributions for ^{31}P and ^{32}S along with the simulated one are shown in Fig. 1a, while the selected angular momentum phase space is shown in Fig. 1b. It should be mentioned here that the selected angular momentum distributions were properly normalized with the input channel fusion cross-section obtained from the PACE4 code for ^{31}P and ^{32}S. It is interesting to note from Fig. 1a that fold distributions for ^{31}P and ^{32}S were the same asserting the fact that the angular momentum populations for both the nuclei were the same.

The experimental spectra were analyzed with a modified version of CASCADE code [33] in which isospin was properly taken care of [16]. Two types of pure isospin states $I_< = I_z$ and $I_> = I_{z+1}$ were considered. The fraction of $\gtrless$ states that mixes with $\lessgtr$ states was defined as [17]

$$\alpha^2_{\gtrless} = \frac{\Gamma^{\downarrow}_{\gtrless}/\Gamma^{\uparrow}_{\gtrless}}{1+\Gamma^{\downarrow}_{\gtrless}/\Gamma^{\uparrow}_{\gtrless}+\Gamma^{\downarrow}_{\lessgtr}/\Gamma^{\uparrow}_{\lessgtr}} \quad (1)$$

where $\Gamma^{\uparrow}$ is the statistical decay width of the CN. The mixed populations of the compound nuclear states were defined as

$$\tilde{\sigma}_< = (1-\alpha^2_<)\sigma_< + \alpha^2_>\sigma_> \quad (2)$$

$$\tilde{\sigma}_> = (1-\alpha^2_>)\sigma_> + \alpha^2_<\sigma_< \quad (3)$$

where $\sigma_<$ and $\sigma_>$ are the population of the pure isospin states. The level density of each type of isospin states was accounted for and the transmission coefficient was divided into isospin dependent and independent parts. The calculation contains only $\Gamma^{\downarrow}_>$ as the free parameter (to be derived from the experimental data). The details of the calculation can be obtained in Ref. [16,34].

The statistical model analysis for ^{31}P was performed with the assumption that the isospin is fully conserved ($\Gamma^{\downarrow}_> = 0$). The CASCADE neutron spectrum (after correcting for detector efficiency) was compared with the experimental spectrum and χ^2 minimization was done in the energy range 4.0–10.0 MeV. The Reisdorf level density prescription [35] was used and the best fit was obtained for $\tilde{a} = 4.2 \pm 0.3$ MeV. Similar analysis resulted in $\tilde{a} = 3.9 \pm 0.1$ for ^{32}S. The evaporated neutron energy spectra along with the CASCADE fit are shown in Fig. 2. In the next step, the IVGDR parameters were extracted by comparing the high energy γ-ray spectrum of ^{31}P with the CASCADE calculations along with a small bremsstrahlung component parametrized as $\sigma = \sigma(0)e^{-E_\gamma/E_0}$. The slope parameter $E_0 = 4.9$ MeV which is consistent with the parametrization $E_0 = 1.1[(E_{lab} - V_c)/A]^{0.72}$ [36]. The deduced parameters were $E_{GDR} = 17.8 \pm 0.2$ MeV, $\Gamma_{GDR} = 8.0 \pm 0.4$ MeV and $S_{GDR} = 1.00 \pm 0.03$. The uncertainties were obtained by χ^2 minimization procedure in the energy range 14–21 MeV. The experimental high energy γ-ray spectrum for ^{31}P along with the CASCADE spectra, properly folded with the detector response function, are shown in Fig. 3a. In order to emphasize on the GDR region the corresponding linearized spectra are shown in Fig. 3b, using the quantity $F(E_\gamma)Y^{exp}(E_\gamma)/Y^{cal}(E_\gamma)$, where $Y^{exp}(E_\gamma)$ and $Y^{cal}(E_\gamma)$ are the experimental and the CASCADE spectra, while $F(E_\gamma)$ is the Lorentzian having the above mentioned parameters.

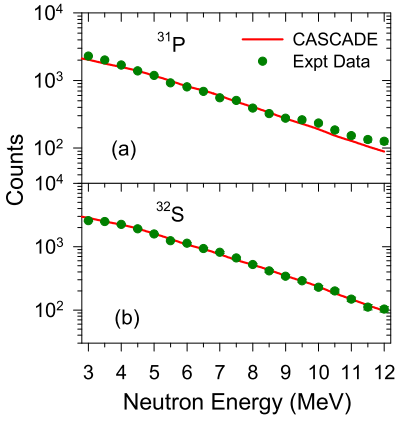

Fig. 2. (Color online.) Experimental neutron spectra (green filled circles) along with the CASCADE predictions (red solid lines) for (a) ^{31}P and (b) ^{32}S.

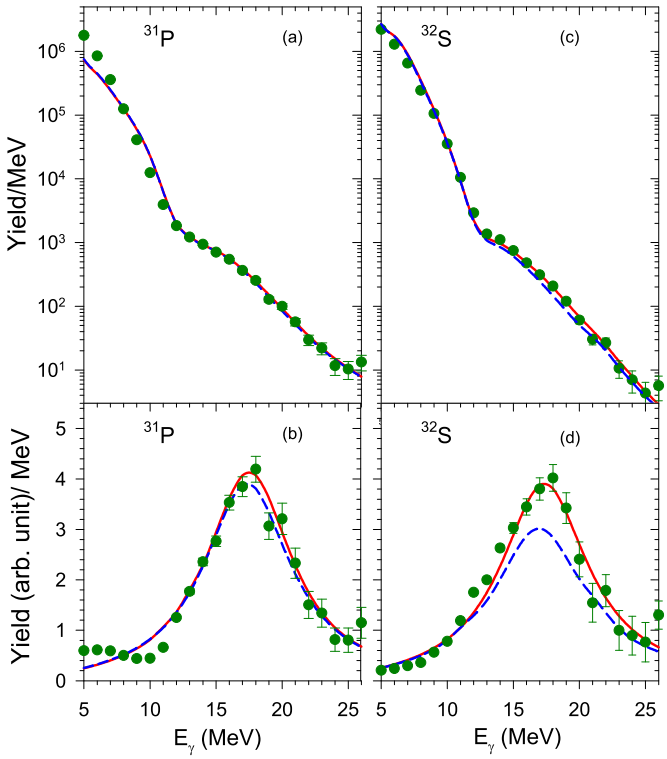

Fig. 3. (Color online.) Experimental high energy γ-ray spectra (green filled circles) along with CASCADE calculations for $\Gamma^{\downarrow}_> = 0$ keV (blue dashed line) and $\Gamma^{\downarrow}_> = 24$ keV (red solid line) for ^{31}P (a) and ^{32}S (c). The corresponding linearized plots are also shown for ^{31}P (b) and ^{32}S (d).

Finally, the isospin mixing parameters were deduced utilizing the IVGDR parameters extracted from ^{31}P. In order to increase the sensitivity of isospin mixing and minimize the effects of statistical model parameters, isospin mixing was deduced from the ratio of γ-ray cross-sections of ^{32}S and ^{31}P in the GDR region (Fig. 4b). We remark here that though we could simulate the response function of LAMBDA spectrometer, the absolute efficiency (ϵ_{in}) of the array is not known. So, we have taken the ratio of $[\sigma_\gamma \times \epsilon_{in}]$ for both the nuclei and compared with the ratio of CASCADE cross-sections properly folded with the detector response function. It should be highlighted here that $\Gamma^{\downarrow}_>$ was the only parameter that was varied to match the experimental ratio with the CASCADE prediction. As $\Gamma^{\downarrow}_>$ remains nearly temperature independent [17,37],

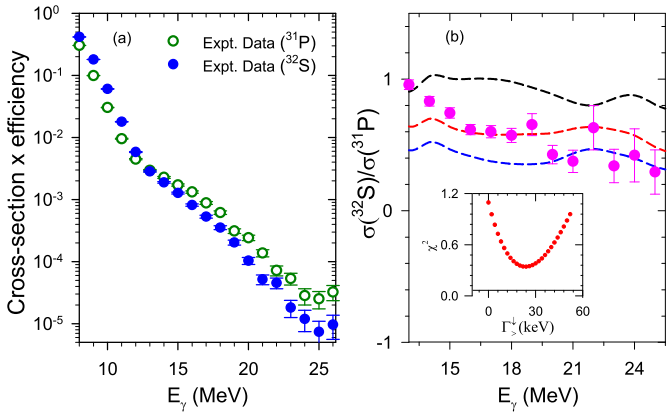

Fig. 4. (Color online.) (a) Experimental $\sigma_\gamma \times \epsilon_{in}$ for ^{31}P (green open circles) and ^{32}S (blue filled circles). (b) Experimental ratio (pink filled circles) of the high energy γ-ray cross-sections of ^{32}S and ^{31}P along with the CASCADE predictions for different $\Gamma^\downarrow_>$. $\Gamma^\downarrow_> = 0$ keV for blue dashed line (zero mixing), $\Gamma^\downarrow_> = 24$ keV for red dashed line and $\Gamma^\downarrow_> = 10$ MeV for black dashed line (full mixing). χ^2 as a function of $\Gamma^\downarrow_>$ (inset Fig. b).

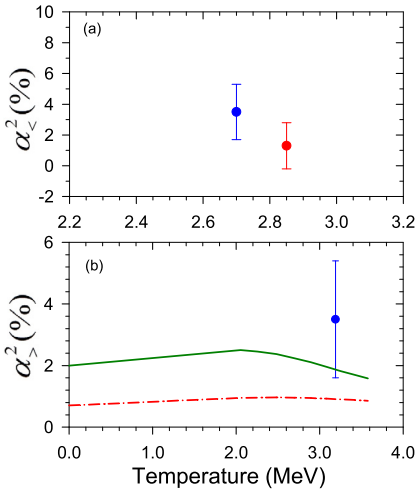

Fig. 5. (Color online.) (a) Measured $\alpha^2_<$ for ^{32}S at different temperatures. The blue solid circle is the present measurement and the red filled circle is adopted from Ref. [24]. (b) Comparison of our measured $\alpha^2_>$ at J = 1$\hbar$ with the calculation of $\alpha^2_>$ with T [6]. $\alpha^2_>$ at T = 0 imposed from Ref. [20] (red dot dashed line), $\alpha^2_>$ at T = 0 calculated using the formalism of Ref. [9] by imposing δ_c value from Ref. [7] (green solid line).

same $\Gamma^\downarrow_>$ was used for all the decay steps. The best value for $\Gamma^\downarrow_>$ was obtained by χ^2 minimization technique in the energy range 14–21 MeV and was found to be 24 ± 13 keV corresponding to $\alpha^2_< = 3.5 \pm 1.8\%$ at T = 2.7 MeV. The experimental high energy γ-ray spectrum for ^{32}S along with the CASCADE fit for $\Gamma^\downarrow_> = 0$ keV and $\Gamma^\downarrow_> = 24$ keV are shown in Fig. 3c and the corresponding linearized plots are shown in Fig. 3d. We emphasize here that the presentations (Fig. 3c and 3d) depend on the normalization point; however, the extracted $\Gamma^\downarrow_>$ from the ratio of the cross sections of ^{32}S and ^{31}P is completely independent of the normalization point. It should be mentioned that $\alpha^2_<$ depends on J and our quoted value corresponds to J = 11$\hbar$, the peak of the J distribution. The temperature was calculated using the relation $T = \sqrt{(E^* - E_{rot} - \Delta_P)/\tilde{a}}$, where E_{rot} is the rotational energy and Δ_P is the pairing energy. We remark here that the quoted errors correspond to the statistical errors as well as the systematic errors owing to the presence of isotopic impurity in the ^{28}Si target and the uncertainty in the determination of bremsstrahlung component.

It is interesting to compare our result with the only reported measurement for ^{32}S [24] for which $\Gamma^\downarrow_>$ was 20 ± 25 keV and $\alpha^2_<$ was 1.3 ± 1.5% at T = 2.85 MeV [21]. It emphasizes the fact that $\Gamma^\downarrow_>$ indeed remains constant with temperature. It is also fascinating to note from Fig. 5a that $\alpha^2_<$ decreases with the increase in temperature. This is owing to the fact that the competition between the time scales associated with the Coulomb spreading width ($\Gamma^\downarrow$) and the compound nuclear decay width ($\Gamma^\uparrow$) leads towards the restoration of isospin symmetry [38,39]. The intrinsic decay width of the compound nuclear state becomes so large as compared to the Coulomb spreading width that the state does not get sufficient time to mix. However in both the cases angular momenta were different and it would be interesting to disentangle the effects of J and T on $\alpha^2_<$. It could also be conjectured that $\Gamma^\downarrow_>$ does not change much with angular momentum.

It would be appealing to compare our measured $\alpha^2_>$ at minimum angular momentum (1$\hbar$) with the calculation of Sagawa et al. [6]. According to the formalism

$$\alpha^2_> = \frac{1}{I_z + 1} \frac{\Gamma_{IAS}}{\Gamma_{CN} + \Gamma_{IVM}} \tag{4}$$

where Γ_{IAS} is the spreading width of IAS, which is equivalent to $\Gamma^\downarrow_>$, Γ_{CN} is the compound nuclear decay width and Γ_{IVM} is the width of the isovector monopole (IVM) state at the energy of IAS. $\alpha^2_>$ was set at 0.7% at T = 0 from the recent calculation of Satula et al. [20]. This results in $\Gamma_{IVM} = 3.4$ MeV as $\Gamma_{CN} = 0$ at T = 0. Next, Γ_{CN} was calculated using the CASCADE code at different temperatures using our best fit parameters. The resulting calculation is shown in Fig. 5b (red dot dashed line). It should be mentioned here that Γ_{IVM} was assumed temperature independent and $\Gamma^\downarrow_>$ was given a weak linear dependence [6] on T as $\Gamma^\downarrow_>(T) = \Gamma^\downarrow_>(0)(1 + cT)$ where $c = 0.2$ MeV^{-1}. The parameter c was calculated by assuming that $\Gamma^\downarrow_>(T = 2.7 \text{ MeV}) = 37$ keV i.e. $\Gamma^\downarrow_>$ remained within the experimental error bar. As can be seen from Fig. 5b that our measured $\alpha^2_> = 3.5 \pm 1.9\%$ remains well above the calculated value.

The value of $\alpha^2_>$ at T = 0 has also been extracted using the calculated value of $\delta_c = 0.65\%$ in ^{34}Cl which reproduces the corrected ft value [7]. $\alpha^2_>$ is extracted utilizing the formalism of Ref. [9] with the assumption that δ_c is same for ^{34}Cl and ^{32}S. According to this formalism $\alpha^2_>$ is defined as

$$\alpha^2_> = \frac{41\xi A^{2/3}}{4(I+1)V_1}\,\delta_c \tag{5}$$

where $V_1 = 100$ MeV, $\xi = 3$ [9]. Equation (5) yields $\alpha^2_> = 2.0\%$ which in turn yields $\Gamma_{IVM} = 1.2$ MeV. $\alpha^2_>$ was extrapolated to higher temperatures using the same procedure described before. As can be seen from Fig. 5b the calculation (solid green line), though underpredicts, better explains our measured data. It should be highlighted in this context that Melconian et al. [40] have found δ_c to be as high as $5.3 \pm 0.9\%$ which was attributed to the presence of close lying I = 0 and I = 1 states near 7.0 MeV excitation energy in ^{32}S and it was corroborated by the shell model calculations. So, it would be interesting to perform the statistical model analysis with the local effects but is beyond the scope of the present work. It should also be highlighted here that, as mentioned therein, the formalism of Sagawa et al. [6] may be valid in medium-heavy and heavy nuclei. However, more data are required at still lower temperatures to understand the systematic behavior of isospin mixing in lower mass region.

In summary, we have measured the isospin mixing in ^{32}S by utilizing α-induced fusion reactions. Precise temperature was determined by simultaneous measurement of NLD parameter and angular momentum. Coulomb spreading width $\Gamma^\downarrow_>$ was found to be

nearly independent of temperature and angular momentum. Moreover, isospin becomes a good quantum number with the increase in temperature. However, $\alpha^2_>$, when extrapolated to higher temperatures, by imposing its value at zero temperature, underpredicts our measured value.

Acknowledgements

The authors would like to thank A. Corsi for providing the isospin included CASCADE code originally obtained from M. Kicinska-Habior. Debasish Mondal sincerely acknowledges the discussions with J.A. Behr.

References

[1] W. Heisenberg, Z. Phys. 77 (1932) 1.
[2] E.P. Wigner, Phys. Rev. 51 (1937) 106.
[3] D.H. Wilkinson, Isospin in Nuclear Physics, North-Holand Publishing Company, Amsterdam, 1969.
[4] J. Janecke, et al., Nucl. Phys. A 463 (1987) 571.
[5] T. Suzuki, et al., Phys. Rev. C 54 (1996) 2954.
[6] H. Sagawa, et al., Phys. Lett. B 444 (1998) 1.
[7] J.C. Hardy, et al., Phys. Rev. C 91 (2015) 025501.
[8] V. Rodin, Phys. Rev. C 88 (2013) 064318.
[9] N. Auerbach, Phys. Rev. C 79 (2009) 035502.
[10] H. Sagawa, et al., Phys. Rev. C 53 (1996) 2163.
[11] E. Farnea, et al., Phys. Lett. B 551 (2003) 56.
[12] N. Severijns, et al., Phys. Rev. C 71 (2005) 064310.
[13] P. Schuurmans, et al., Nucl. Phys. A 672 (2000) 89.
[14] Vandana Tripathi, et al., Phys. Rev. Lett. 111 (2013) 262501.
[15] M.N. Harakeh, et al., Phys. Lett. B 176 (1986) 297.
[16] J.A. Behr, et al., Phys. Rev. Lett. 70 (1993) 3201.
[17] H.L. Harney, et al., Rev. Mod. Phys. 58 (1986) 607.
[18] A. Corsi, et al., Phys. Rev. C 84 (2011) 041304(R).
[19] S. Ceruti, et al., Phys. Rev. Lett. 115 (2015) 222502.
[20] W. Satula, et al., Phys. Rev. Lett. 103 (2009) 012502.
[21] M. Kicinska-Habior, Acta Phys. Pol. B 36 (2005) 1133.
[22] A. Bracco, et al., Phys. Rev. Lett. 74 (1995) 3748.
[23] Deepak Pandit, et al., Phys. Rev. C 81 (2010) 061302(R).
[24] M. Kicinska-Habior, et al., Nucl. Phys. A 731 (2004) 138.
[25] S. Mukhopadhyay, et al., Phys. Lett. B 709 (2012) 9.
[26] Deepak Pandit, et al., Phys. Lett. B 713 (2012) 434.
[27] Balaram Dey, et al., Phys. Lett. B 731 (2014) 92.
[28] Dimitri Kusnezov, et al., Phys. Rev. Lett. 81 (1998) 542.
[29] S. Mukhopadhyay, et al., Nucl. Instr. Meth. A 582 (2007) 603.
[30] K. Banerjee, et al., Nucl. Instr. Meth. A 608 (2009) 440.
[31] R. Brun, et al., GEANT3, CERN-DD/EE/84-1, 1986.
[32] Deepak Pandit, et al., Nucl. Instr. Meth. A 624 (2010) 148.
[33] F. Puhlhofer, Nucl. Phys. A 280 (1977) 267.
[34] J.A. Behr, Ph.D. thesis, University of Washington, 1991, unpublished.
[35] W. Reisdorf, et al., Z. Phys. A 300 (1981) 227.
[36] H. Nifennecker, et al., Annu. Rev. Nucl. Part. Sci. 40 (1990) 113.
[37] E. Kuhlmann, Phys. Rev. C 20 (1979) 415.
[38] H. Morinaga, Phys. Rev. 97 (1955) 444.
[39] D.H. Wilkinson, Philos. Mag. 1 (1956) 379.
[40] D. Melconian, et al., Phys. Rev. Lett. 107 (2011) 182301.